CrystEngComm

ROYAL SOCIETY OF CHEMISTRY

PAPER

View Article Online
View Journal | View Issue

Cite this: *CrystEngComm*, 2023, **25**, 5001

Encapsulation of N-containing compounds in a new hydrophilic Cd-based crystalline sponge *via* coordinative alignment method†

Faiza Habib, * Derek A. Tocher and Claire J. Carmalt

The crystalline sponge method (CSM) is a technology which allows precise molecular determination of non-crystalline compounds, without the need to crystallise them independently, by soaking them in a crystalline metal–organic framework (MOF). To expand the CSM to a wider range of guest molecules, the development of a new crystalline sponge is essential. In this study a new Cd-based MOF $\{[Cd_7(4,4'4''$-[1,3,5-benzenetriyltris(carbonylimino)]-trisbenzoato)$_4(\mu_3$-OH)$_2(H_2O)_4(DMF)_4]\cdot(solvent)_x\}_n$ was synthesized and investigated as an alternative crystalline sponge (**2**). Sponge **2** demonstrated versatility in solvent stability compared to the well-studied $[\{(ZnI_2)_3$(tris(4-pyridyl)-1,3,5-triazine$)_2\cdot x(CHCl_3)\}_n]$ (**1**) and was stable in the presence of polar aprotic, polar protic solvents and Lewis bases. Inclusion complexes with three solvents, acetonitrile, acetone, and isopropanol were prepared. These guest molecules were fixed in the pore *via* hydrogen bonding confirming the hydrophilic pore environment of sponge **2**. Notably, sponge **2** also demonstrated the ability to accommodate N-containing compounds such as pyridine, 3,5-lutidine, and 4-aminopyridine *via* the coordinative alignment method (CAL). A study was conducted to compare the ability of sponge **2** and related pyridine containing sponge **3** by encapsulating the same pair of guests: *N*, *N*-dimethylaniline and propiophenone.

Received 13th June 2023,
Accepted 4th August 2023

DOI: 10.1039/d3ce00592e

rsc.li/crystengcomm

1. Introduction

The crystalline sponge method (CSM) was first introduced in 2013 by Fujita and co-workers,[1] for the structural determination of non-crystalline compounds by single crystal X-ray diffraction (SCXRD). SCXRD is recognised as the most reliable analytical technique in structure determination. However, a fundamental limitation of this method is the requirement for high-quality single crystals. The 'crystalline sponge' technology removed the need to obtain single crystals of the compound of interest and allowed the analysis of powder, amorphous solid, liquid, volatile matter, or oily state material *via* SCXRD. The CSM, involves using a porous framework material such as a metal–organic framework (MOF), as a host 'crystalline sponge' to absorb the non-crystalline compounds (referred to as guests hereafter) into its pores. These guest compounds are arranged through host–guest interactions arranged in a regular pattern and thus contribute to the Bragg peaks and a characteristic diffraction pattern. Hence, the structure of the guests can be determined along with the host framework by SCXRD.

Since this technique was introduced, the method has been applied to a number of research fields for the structure determination of compounds that are difficult to isolate and/or are produced in minute quantities.[2–5] For example, in synthetic organic chemistry structure determination of metabolites,[2,6,7] reaction intermediates[8–10] and short-lived species,[11] were possible by applying the CSM. In addition, several reaction mechanisms were studied by utilising the CSM technique.[12–14] For example, the mechanism of Pd-catalysed aryl bromination[15] was studied. The CSM can also be applied to compounds present in nanogram-microgram quantities. Hence, the CSM has been especially appealing for absolute structure determination of several mass-limited natural products.[3,16–19] Several industries and pharmaceutical companies are currently using the CSM for the structure determination of active pharmaceutical ingredients in the drug development process.[20–23] The structure elucidation of any dangerous metabolites is essential before the drug is tested on patients. In summary the CSM is an emerging technology and is developing rapidly with new applications. This technology has the potential to impact several research areas and maybe even revolutionise entire industries.

Although, the Zn-MOF, $[\{(ZnI_2)_3$(tris(4-pyridyl)-1,3,5-triazine$)_2\cdot x(CHCl_3)\}_n]$ (**1**) is the most common and successful

Department of Chemistry, University College London, 20 Gordon Street, London, WC1H 0AJ, UK. E-mail: faiza.habib@ucl.ac.uk, faizahabib.amu@gmail.com, d.a.tocher@ucl.ac.uk, c.j.carmalt@ucl.ac.uk

† Electronic supplementary information (ESI) available: CCDC 2240137, 2240138 and 2243754–2243762. For ESI and crystallographic data in CIF or other electronic format see DOI: https://doi.org/10.1039/d3ce00592e

crystalline sponge, it has practical limitations such as the hydrophobic pore environment, small pore size, and instability in the presence of polar solvents and nucleophiles. Therefore, the range of guest molecules found in sponge **1** is limited. Hence, to expand the CSM to a wider range of guest molecules, the development of alternative crystalline sponges is essential. Several researchers have developed a variety of crystalline sponges[19,24,25] based on porous organic MOFs,[26–28] chiral metal–organic materials,[29–32] hydrophilic MOFs,[33,34] coordination cages,[35] and biological frameworks.[36] All of these alternative sponges were developed to overcome the limitations of sponge **1** and each to target a particular type of guest encapsulation. The hydrophobicity issue was addressed by several researchers in previous studies and hydrophilic sponges have been developed to encapsulate hydrophilic guest compounds.[33,37] However, relatively less attention has been paid to the incompatibility of crystals of sponge **1** with polar solvents and nucleophilic guests. For example, the framework of sponge **1** was severely damaged when exposed to nicotine and therefore cannot be studied by SCXRD.[38] In the literature a few crystalline sponges have demonstrated the compatibility with nucleophilic guests.[26,39] A Mn-based coordination porous framework – 5 (CPF-5) binds several Lewis base guests, including pyridine by coordinative alignment.[40] In addition, a hydrophilic Gd-MOF also demonstrated stability in polar solvents.[33]

In this work a new versatile MOF was synthesised which addresses all three limitations of **1** described above. A Cd-based MOF $[Cd_{1.5}$(4,4′4″-[1,3,5-benzenetriyltris(carbonylimino)]-trisbenzoato)$(H_2O)(DMF)]\cdot(solvent)_x$ was selected from literature as a potential crystalline sponge.[41] Modification of the synthetic procedure led to the formation of a new framework $[Cd_7$(4,4′4″-[1,3,5-benzenetriyltris(carbonylimino)]-trisbenzoato)$_4(\mu3\text{-}OH)_2(H_2O)_4(DMF)_4]\cdot(DMF)_7$ (MOF **2**) which was then used in this study. The crystal structure was also found different from that reported previously. It was observed that MOF **2** was crystallised in the monoclinic $P2_1/n$ space group instead of triclinic $P\bar{1}$. The original structure was a two-dimensional framework generated from the linking of trimeric cadmium clusters with BTA^{3-} bridges. The asymmetric unit consisted of one BTA^{3-} linker and two Cd^{2+} ions, and each Cd^{2+} ion was six coordinate. However, the structure obtained in this work exhibited a two-fold interpenetrating three-dimensional honeycomb framework. MOF **2** have several structural features which are essential to the use a crystalline sponge. First, **2** crystallises in the low symmetry monoclinic $P2_1/n$ space group, which reduces the chance of a guest molecule being located on a symmetry element (thus leading to disorder). Second, **2** exhibited large pore dimensions of 10 × 16 $Å^2$, larger than **1**. Therefore, larger guest molecules can be accommodated in **2**. Third, the 4,4′4″-[1,3,5-benzenetriyltris(carbonylimino)]-trisbenzoic acid (H_3BTA) linker having free carbonyl groups would contribute to a hydrophilic pore environment by fixing the incoming guest molecules *via* hydrogen bonding. In addition, the dimethylformamide (DMF) solvent molecules were bonded to the Cd^{2+} ions and may be replaced by the guest molecules and hence **2** can accommodate guests *via* the coordinative alignment method. With all these features it was determined that MOF **2** would be an ideal candidate for use in the CSM. To determine usability, MOF **2** was exposed to several solvents including polar aprotic, polar protic solvents and Lewis bases. MOF **2** demonstrated outstanding stability in variety of solvents. Guests were encapsulated in the pores of MOF **2** and N-containing compounds were accommodated by CAL to the Cd.

2. Results and discussion

Structure of $\{[Cd_7$(4,4′4″-[1,3,5-benzenetriyltris(carbonylimino)]-trisbenzoato)$_4(\mu3\text{-}OH)_2(H_2O)_4(DMF)_4]\cdot(DMF)_7\}$ MOF 2

MOF **2** crystallised in the monoclinic $P2_1/n$ space group. The asymmetric unit of MOF **2** consists of seven Cd^{2+} ions, four linker molecules, two triply bridged hydroxide ion (μ_3-OH), four coordinated DMF molecules shown in magenta in Fig. 1 and four coordinated water molecules bonded to Cd^{2+} ions. In addition, six DMF molecules were identified and refined in the pores, shown in blue in Fig. 1. The triply bridging oxygen was assigned as hydroxide ion on the basis of metal–oxygen bond length which is 2.21 to 2.35 Å. A typical Metal-hydroxide bond length varies from 1.98 to 2.35 Å. Therefore, Cd–OH bond length falls within the range. In addition, the bridging hydroxide ion typical form a tetrahedral geometry and Fig. S1(i)† is showing Cd–O–Cd bond angle of 109.80°. All these evidences strongly suggestive that triply bridging oxygen is a hydroxide ion. Further, presence of two hydroxide ion balances the charge on MOF **2**. Each cadmium ion bridges three BTA^{3-} linker molecules, and each BTA^{3-} linker molecule further connects three neighboring cadmium ions to form a three-dimensional, double interpenetrated honeycomb framework, as shown in Fig. 2. In topology, the framework of **2** can be simplified as (3,6)-network when one SBU connects six linkers and one linker joins three SBUs. The Cd^{2+} ions of **2** are six coordinate with an octahedral

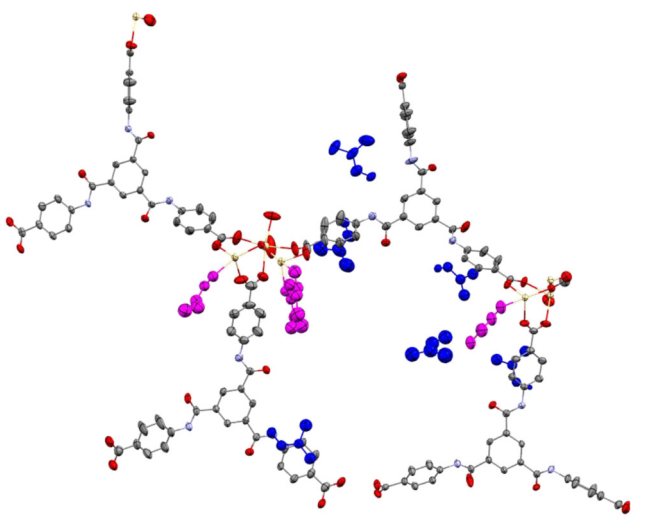

Fig. 1 Asymmetric unit of sponge **2**. Framework shown in ellipsoids with 50% probability. DMF molecules in the pore shown in blue and DMF coordinated to Cd ions are shown in magenta.

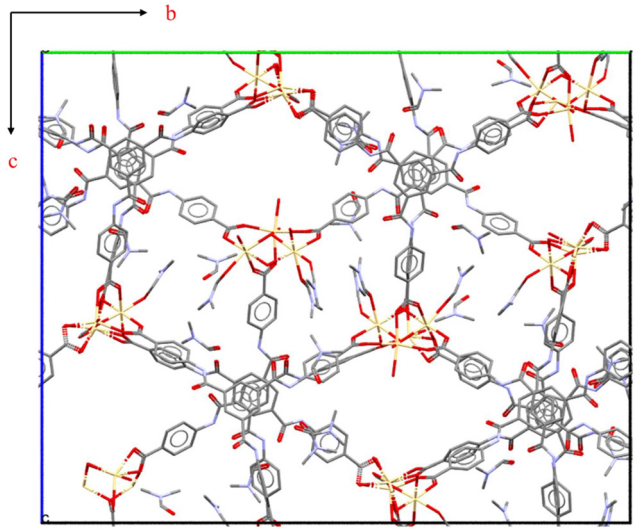

Fig. 2 Cell packing diagram for **2** viewed down the *a*-axis.

geometry bonded to six oxygen atoms, except Cd 3 which has distorted octahedral geometry. The source of oxygen atoms coordinated to the Cd^{2+} ions varied in the structure. For example, in Cd6 (Fig. S1†) two oxygen atoms are from the two different BTA^{3-} linker molecules, two from the μ_3-OH and the remaining two were from coordinated water and DMF. In contrast, Cd5 (Fig. S1†) is connected to three oxygen atoms from the BTA^{3-} linker, two water molecules, and one μ_3-OH. This difference is probably a function of the number of solvent molecules coordinated to Cd^{2+} ions.

Stability of 2 in a range of solvents

MOF **2** was exposed to a variety of solvents containing different chemical functionalities to establish its practical stability before exposure to the guest of interest.[42] The results were compared with the reported solvent stability of sponge **1** and with the Gd-MOF previously reported,[33] which was reported with better stability than sponge **1**. If the host crystals of MOF **2** survived after 1–2 days of exposure to a particular solvent and a crystal structure was obtained, then it was considered to be stable in that solvent. In contrast, if the crystals were damaged after 1–2 days of exposure and did not diffract, then instability with regard to that solvent was concluded. The results summarized in Table 1 revealed that MOF **2** was stable in most of the solvents studied except methanol and chloroform. It was clear that MOF **2** demonstrated a wide range of stability. In addition, the stability of **2** in polar solvents and basic solvents was similar to that of the Gd-MOF. Even though the crystals of **2** deteriorated in methanol and chloroform, they proved sufficiently stable in many solvents for the application of the CSM. The outstanding stability of **2** demonstrates the potential to encapsulate polar and nucleophilic guest molecules.

Encapsulation of solvents in pores of 2

The crystals of **2** were found stable in acetonitrile (**A**), acetone (**B**) and isopropanol (**C**) up to 1 month without showing any sign of deterioration. The inclusion complexes with these solvents were isolated (**2A**, **2B** and **2C**) after soaking crystals of **2** at 25 °C with the neat solvents (hereafter referred to as guests) to obtain high occupancies.[42] The soaking period was optimised to give the maximum occupancies as well as the best quality crystals for X-ray diffraction measurements (details of soaking experiment are available in ESI† Table S1). The results revealed that the framework structure of the inclusion complexes **2A**, **2B** and **2C** was unchanged from the structure of **2**. The structure of all inclusion complexes contains seven Cd^{2+} ions and four BTA^{3-} linkers and crystallised in the $P2_1/n$ space group as with **2**. All inclusion complexes show slight differences in unit cell parameters (Table S4†). Detailed analysis of all three inclusion complexes revealed that these guest molecules did not replace DMF molecules from the coordination sites and only occupied sites in the pore. In addition, a few DMF molecules remained in the pore. It was important to remove DMF and water molecules to facilitate successful guest exchange and to make sure that the maximum number of sites were available for the incoming guests. In other work solvents such as methanol was used to replace DMF successfully from the pores and coordination sites.[43] This method was successful for the removal of DMF from MOF **2**. However, a few DMF remained in pore because they were strongly bonded to the framework *via* hydrogen bonding (Fig. S2†).

Structures of 2A, 2B and 2C

Fig. 3a illustrates the packing diagram of MOF **2** and all DMF molecules both coordinated to Cd ions and in the pore are

Table 1 Stability of MOF **2** in solvents in comparison with sponge **1** and Gd-MOF

Solvent	MOF **2**[this work]	**1** (ref. 1)	Gd-MOF[33]
Methanol	Deteriorated	Deteriorated	Survived
Ethanol	Survived	Not reported	Not reported
Isopropanol	Survived	Not reported	Not reported
Acetone	Survived	Survived (in diluted acetone)	Not reported
Chloroform	Deteriorated	Survived	Survived
DMF	Survived	Deteriorated	Survived
Acetonitrile	Survived	Deteriorated	Survived
Pyridine	Survived (in diluted pyridine)	Deteriorated	Survived

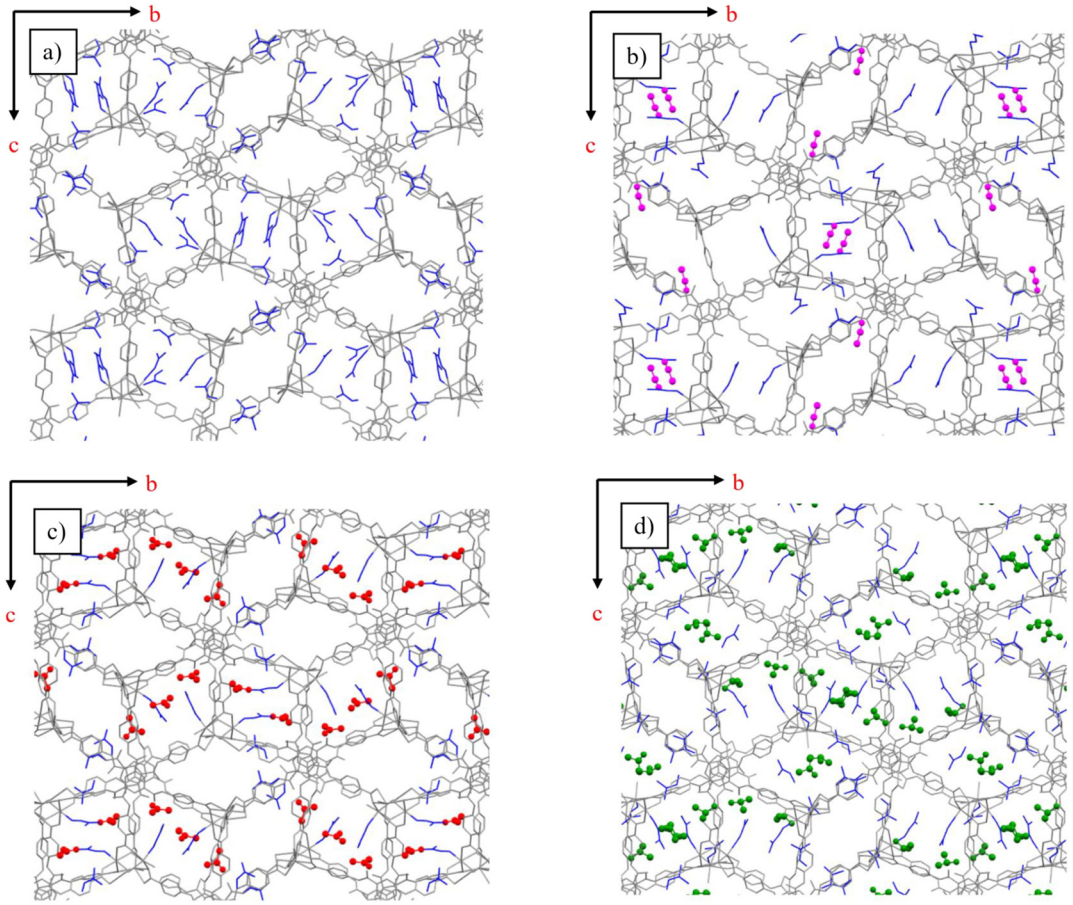

Fig. 3 a) Packing diagrams viewed down the *a*-axis of a) sponge **2** b) inclusion complex with acetonitrile, c) acetone, d) isopropanol. Framework is displayed in capped stick and guest molecules in ball and stick.

shown in blue. Fig. 3b–d show the packing diagrams of the inclusion complexes **2A–2C** respectively. The DMF molecules in inclusion complexes **2A–2C** are also shown in blue as capped stick and the guests are shown as ball and stick models. The positions of the guest molecules **A–C** in the pores were studied and compared to gain an insight into the dominant host-guest interactions. It was observed that only a few guest molecules were found at the site of DMF molecules in **2** and the remaining guests occupy unique sites. However, all the guests **A**, **B**, **C** and DMF were fixed in place *via* hydrogen bonding demonstrating hydrophilic pore environment of **2**. (Detailed diagrams of host-guest interactions of **2A**, **2B** and **2C** can be observed in ESI† section S3).

Encapsulation of N-containing compounds *via* coordinative alignment method

In contrast to the results obtained with **A**, **B** and **C**, encapsulation of pyridine resulted in replacement of all the DMF molecules bonded to Cd^{2+} ions by the new guest. Initially, crystals of **2** were soaked in neat pyridine which led to rapid loss of all crystalline material, presumably due to nucleophilic substitution at many (all) of the Cd coordination sites. Therefore, pyridine was diluted with acetone before soaking resulting in the formation of good quality crystals. Details of solvent exchange and optimisation conditions are presented in Table S1 in the ESI.† This result encouraged us to further encapsulate nucleophilic guests in **2** and to explore the guest encapsulation by coordinative alignment. 3,5-Lutidine (**D**) and 4-aminopyridene (**E**) (Fig. 4a and b) were selected as guest candidates and as expected these guests were accommodated *via* the CAL method. All three of the inclusion complex **3**, **2D** and **2E** crystallised in the same $P2_1/n$ space group, as **2**.

Inclusion complex 3

There are nine pyridine molecules observed in the asymmetric unit of **3**. Eight of them are coordinated to Cd^{2+} ions shown in orange, and one was observed in the pore, shown in turquoise with 50% occupancy. Fig. 5a illustrates the packing diagram of the inclusion complex **3**. Two DMF molecules in blue and three acetone molecules in red (used for diluting pyridine for soaking) were found in the pore as well. The structure of the inclusion complex **3** with seven Cd^{2+} ions and four BTA^{3-} linkers is different from **2** in that pyridine was found coordinated to the Cd^{2+} ions replacing all the coordinated DMF from **2**, and hence the structure of sponge **3** is different.

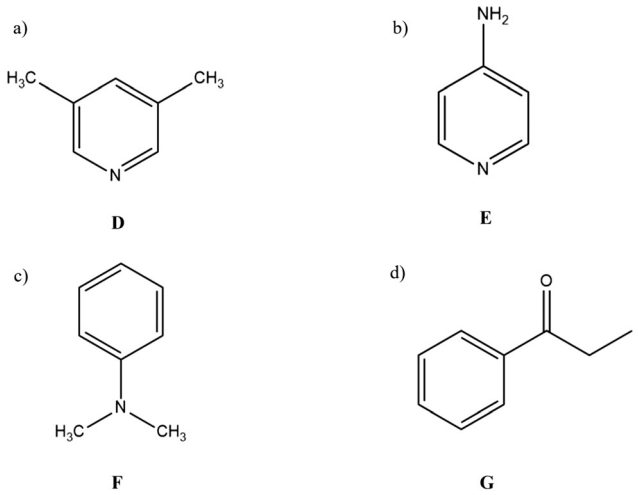

Fig. 4 Guest molecules chosen for encapsulation in **2** a) 3,5-lutidine b) 4-aminopyridine c) *N*,*N*-dimethylaniline d) propiophenone.

Fig. 5b illustrates the pyridine in the pore observed very close to Cd7 but did not coordinate. In addition, the distance between Cd7 and the nitrogen atom of this pyridine was 2.81 Å, which is longer than the coordinated pyridine to Cd^{2+} ion distances, which range from 2.25 to 2.35 Å. However, a short contact between the N of pyridine (shown in turquoise) with the carboxylate of the framework was observed at 2.61 and 2.78 Å. Fig. S6† illustrates the geometry of all the Cd^{2+} ions of **3**. It was observed that the Cd^{2+} ions in **3** were six coordinate, similar to **2**, with octahedral geometry except for Cd3 which has distorted octahedral geometry (Fig. S6c†). Cd^{2+} ions in **3** are now bonded to nitrogen atoms from the pyridine molecule along with the oxygen atoms from the linker molecules and the μ_3-OH. For example, Cd5 is now coordinated to three pyridine molecules. In contrast, Cd5 in **2**, these sites were occupied by two water molecules and one carboxylate from the linker (Fig. S6e†).

Inclusion complex 2D

Fig. 6a show packing diagram of **2D**. Eight 3,5-lutidine molecules were identified in the asymmetric unit of **2D**. Seven of them were bonded to Cd^{2+} ions shown in light green colour and one molecule of 3,5-lutidine was observed in the pore shown in brown colour with 100% occupancy. Three DMF molecules were observed in the pore (shown in blue). In addition, no acetone molecules were found in the pore for this structure because the soaking experiment was performed with the neat guest.

On comparing the structure **2D** with **3**, one difference was identified at Cd5 as in this structure two guest molecules were clearly bonded to the metal, whereas in **3** there were three guest molecules bonded to Cd5. However, in the X-ray analysis there is a significant electron density, which appears to be from a highly disordered 3,5-lutidine molecule at the sixth coordination site on Cd5. All attempts to model this were unsuccessful. In addition, on comparing the geometry of Cd5 from **3**, it was observed that both Cd5 ions have typical octahedral angles with an O–Cd–O angle of 90°. This is consistent with the fact that Cd5 in **2D** has octahedral geometry, and the sixth ligand was severely disordered.

The 3,5-lutidine molecules bonded to Cd5, as shown exhibit orientational disorder and as does the 3,5-lutidine on Cd2. Each was refined across two positions, Fig. S13.† The 3,5-lutidine in the pore forms a hydrogen bond with the framework, $N_{guest}\cdots C_{framework}$ 2.9 Å in **2D**. This result supports the idea that the hydrophilicity of sponge **2** was also a strong reason for the accommodation of Lewis bases.

Inclusion complex 2E

Fig. 6b shows the packing diagram of **2E**. As with pyridine and 3,5-lutidine, 4-aminopyridine replaced all the coordinated DMF molecules from **2** in **2E**. In the asymmetric unit, eight molecules

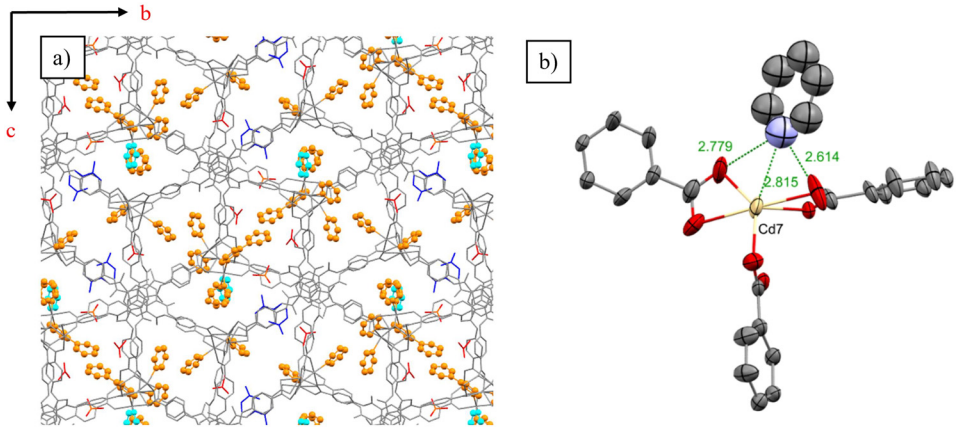

Fig. 5 a) Packing diagram of inclusion complex **3** viewed down the *a*-axis. Framework is shown as capped stick model in grey colour and DMF in blue acetone in red. Guests shown in ball and stick model coordinated pyridine in orange colour and pore pyridine in turquoise colour. b) Interaction between pyridine in the pore of sponge **3** and the framework. Framework and pyridine molecule is displayed in ellipsoids with 50% probability. Interaction distances are displayed in angstroms.

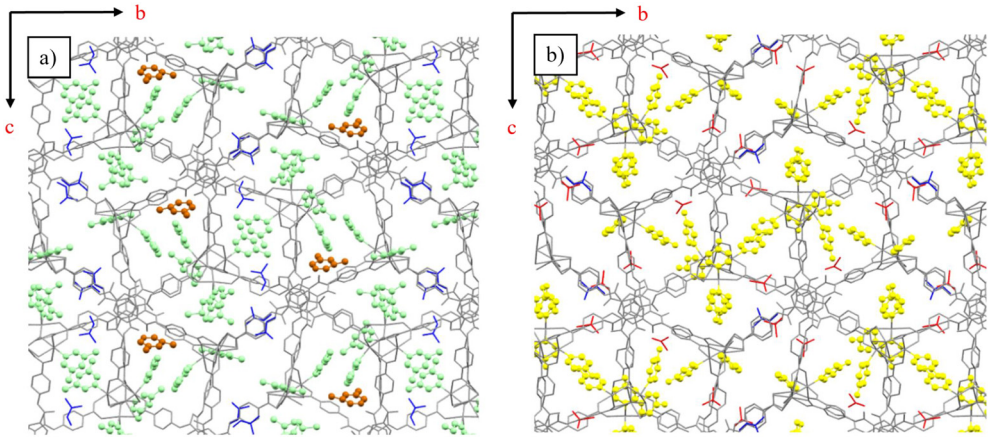

Fig. 6 Packing diagrams of inclusion complexes viewed down the *a*-axis a) **2D**, coordinated 3,5 lutidine is shown in green and pore 3,5 lutidine in brown. b) **2E**, 4-aminopyridine in yellow colour. Framework is shown as capped stick model in grey colour. DMF in blue and acetone in red colour. Guests shown in ball and stick model.

of 4-aminopyridine were identified bonded to Cd^{2+} ions and none were observed in the pores. A DMF molecule and four acetone molecules were however identified in the pore.

Eight molecules of 4-aminopyridine were observed bonded to Cd^{2+} ions. Cd5 was bonded to three molecules of 4-aminopyridine similar with the inclusion complex with pyridine **3**. Comparing the packing diagram of **2E** (Fig. 6b) with that of **3** (Fig. 5a) similarities in the positions of the guest molecules with only slight rotational differences were observed. The 4-aminopyridine molecule on Cd4 showed rotational disorder and atoms were refined across two positions (Fig. S15†).

The 4-aminopyridine molecules interacted with the framework *via* hydrogen bonding. For example, the amino group of the 4-aminopyridine molecule bonded to Cd4 can be seen to be interacting with the carboxylates of the framework *via* a hydrogen bond, $H_{guest}\cdots C{=}O_{framework}$ 3.05 Å, as shown in Fig. 7a. Similarly, the molecule bonded to Cd5 formed hydrogen bonds with the framework, $H_{guest}\cdots C{=}O_{framework}$ 2.90 and 2.80 Å (Fig. 7b). Furthermore, the molecule bonded to Cd6 formed

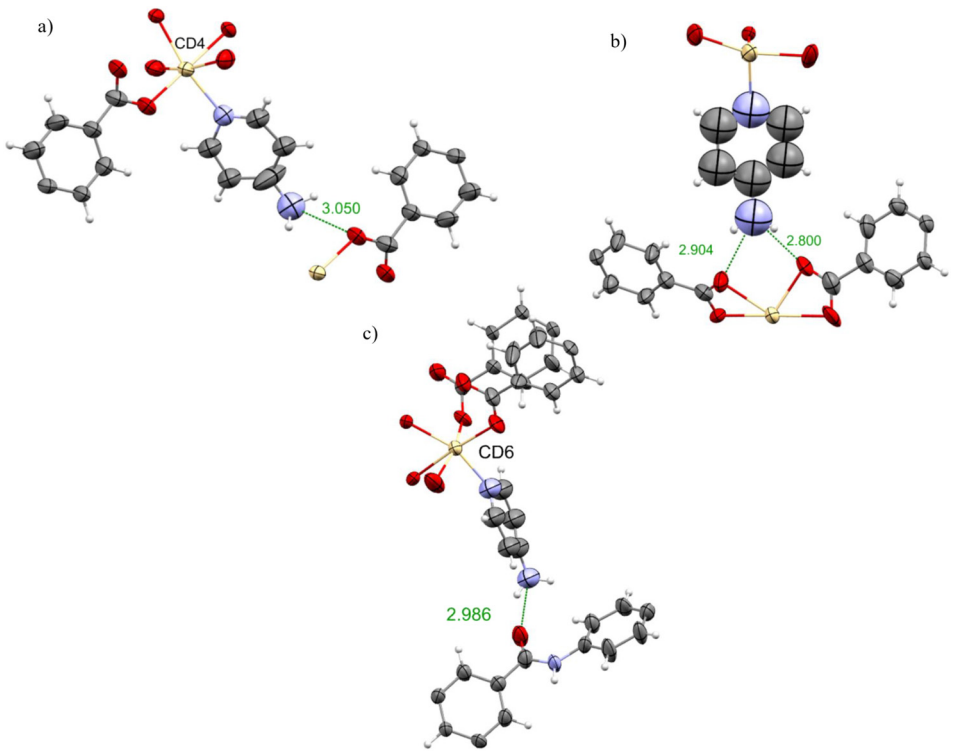

Fig. 7 Intermolecular interactions between molecules of 4-aminopyridine a) bonded to Cd4 b) bonded to Cd5 c) bonded to Cd6 and the host framework. Host framework and guest molecules displayed as ellipsoids with 50% probability. Interaction distances are displayed in angstroms.

hydrogen bonds with the framework $H_{guest}\cdots C{=}O_{framework}$ 2.98 Å, as shown in Fig. 7c. Such interactions were expected because of the hydrophilic nature of the framework. This result was contrasted with the inclusion complex of the Mn-based MOF (CPF-5) with 3-aminopyridine where the 3-aminopyridine[40] was bonded to Mn^{2+} ions *via* CAL and formed hydrogen bonds with other molecules of 3-aminopyridine but not with the framework. In **2E** the remaining five 4-aminopyridine guests form weaker hydrogen bonds with the framework as the $-NH_2$ functional groups were located deep into the pore away from the framework.

Encapsulation of compounds in the pore

Sponge **2** demonstrated the ability to accommodate guests in the pore and also *via* the CAL method. It was noted that the structure of all the inclusion complexes generated from **2**, were closely similar to sponge **2**. For example, sponge **2** and inclusion complex **3** only differ in having DMF and pyridine bonded to the Cd^{2+} respectively. This section of the study attempts to compare sponges **2** and **3** by encapsulating the same pair of guest molecules in both the frameworks and to look for any differences in the interaction with the framework. It was observed that pore solvent molecules, DMF and acetone were fixed by hydrogen bonding as the dominant interaction. Therefore, it was expected that the new guest molecules in **2** might occupy similar sites and be fixed by hydrogen bonding. However, for **3**, it was hoped that due to the presence of pyridine, new guest molecules might align themselves *via* π–π interactions with the pyridine ring.

Two guest molecules were selected for this study, namely *N*, *N*-dimethylaniline (**F**) and propiophenone (**G**) (Fig. 4c and d). These molecules were selected as guests which would not coordinate to the metal centres of the sponges. Therefore, it was expected that this guest will organise itself in the pore. Propiophenone has a ketone group present, however, previous inclusion complex **2B** with acetone shows no coordination with the metal centres of **2**. Therefore, it is likely that propiophenone molecules will be found only in the pores of both the sponges. Nevertheless, in the literature, a few molecules containing the carbonyl/keto group were reported coordinated to metal centres. For example, *e*-caprolactam, *N*-methylcaprolactam[33] and benzyl acetate[44] were observed bonded to the Gd centre *via* the carbonyl group of the guest molecules. Therefore, it was of interest to observe how propiophenone guests would align themselves in the pores of sponges **2** and **3**.

Inclusion complexes with *N*,*N*-dimethylaniline in sponges 2 and 3

The structure of **2F** was similar to that of **2** as DMF is bonded to Cd^{2+} ions in both structures. The unit cell dimensions of **2F** are closely similar to those of **2**. This observation also holds for **3F** and **3** (Table S6†). This result is consistent with all the inclusion complexes previously discussed.

In inclusion complex **2F**, two molecules of *N*,*N*-dimethylaniline were observed in the asymmetric unit, shown purple and lime in Fig. 8a. On the other hand, the inclusion complex **3F** was only able to accommodate one molecule of the *N*,*N*-dimethylaniline shown in purple (Fig. 8b). This might be because a diluted solution of *N*,*N*-dimethylaniline was used to obtain **3F** whereas neat *N*,*N*-dimethylaniline used to obtain **2F**. This is consistent with the observation that the solvent-accessible void space of **2** was 18.6% while that of **3** was 9% of the unit cell volume. It could be noted however that both **2F** and **3F** also have DMF (**2F**) or DMF/acetone (**3F**) in the pores.

In **2F** one molecule of *N*,*N*-dimethylaniline was engaged in a CH–π interaction with the centroid of the aromatic ring of the framework, $CH_{guest}\cdots centroid_{framework}$ 2.78 Å, and also a weak hydrogen bond with a carboxylate of the framework, Fig. 9a. However, the second molecule in the pore had very weak interaction (>4 Å) with the framework structure. Similarly, in inclusion complex **3F**, the only *N*,*N*-dimethylaniline molecule in

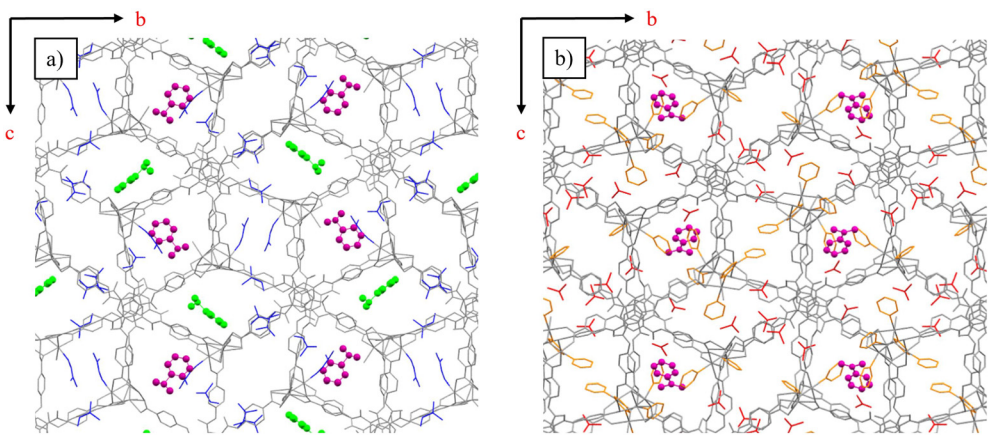

Fig. 8 Packing diagrams of complexes viewed down the *a*-axis. a) **2F**, N,N-dimethylaniline in **2** b) **3F** *N*,*N*-dimethylaniline in **3**, guest molecules were coloured according to their positional equivalence in sponge **2** and **3**. Framework displayed as capped stick in grey colour. DMF in blue, pyridine in orange and acetone in red. Guest molecules as ball and stick representations.

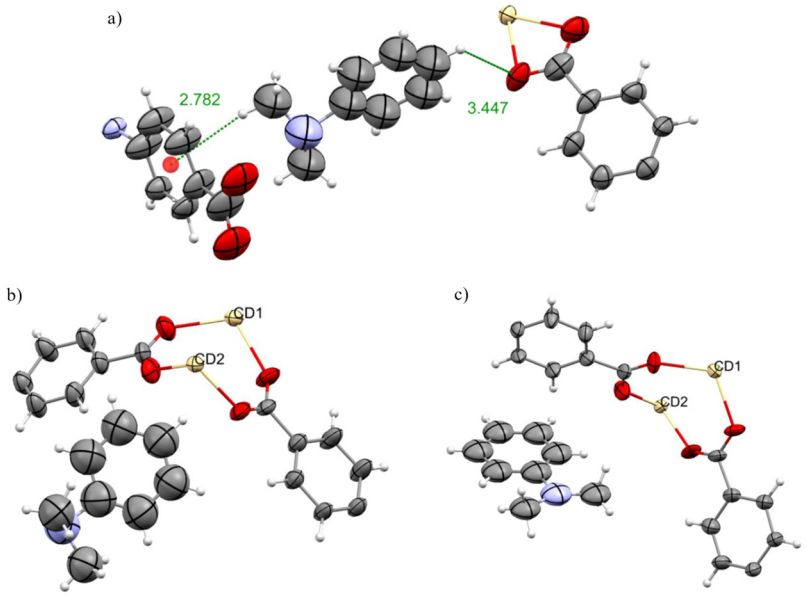

Fig. 9 a) and b) Intermolecular interactions between molecules of *N*,*N*-dimethylaniline in the pore and framework **2**. c) Intermolecular interactions between *N*,*N*-dimethylaniline molecule and framework **3**. Framework and guest molecules displayed as ellipsoids with 50% probability. Interaction distances are displayed in angstroms.

the pore and only weak (>4 Å) interaction with the framework was observed. Fig. 9b and c illustrate the orientation of the molecule of *N*,*N*-dimethylaniline with respect to the framework in **2F** and **3F**, and is quite different in each cases. Interestingly, the sites occupied by the molecules of *N*,*N*-dimethylaniline in both the frameworks are unique and were not occupied by guests in previous structures. Surprisingly, in **2F** the hydrogen bonding was not dominant. In **3F** the pyridine on Cd^{2+} extends into the pore space and it was expected that it would provide an opportunity for π–π bonding to aromatic guests. However, that was not observed in practice. In literature, the inclusion of aniline in a POM based crystalline sponge was reported.[28] In that sponge the aniline molecules were also located deep inside the pore and weaker hydrogen bonding with the framework was observed.

Inclusion complexes of propiophenone with sponges 2 and 3

The inclusion complexes **2G** and **3G** have similar structures to sponges **2** and **3** respectively. Unsurprisingly the unit cell dimensions of **2G** are similar to those of **2**, and the dimension of **3G** is similar to **3** (Table S6†) as reported for all the complexes in this paper.

In the inclusion complex **2G**, four molecules of propiophenone were observed, shown in pink, violet, black and mustard colour Fig. 10a. In contrast, the inclusion complex **3G** has only one propiophenone molecule in the pore, as shown in teal colour in Fig. 10b. The explanation for this parallels that for **2F**/**3F**.

In **2G**, the guest molecule shown in Fig. 11a was observed near the Cd5 ion and it is interacting with the carboxylates of

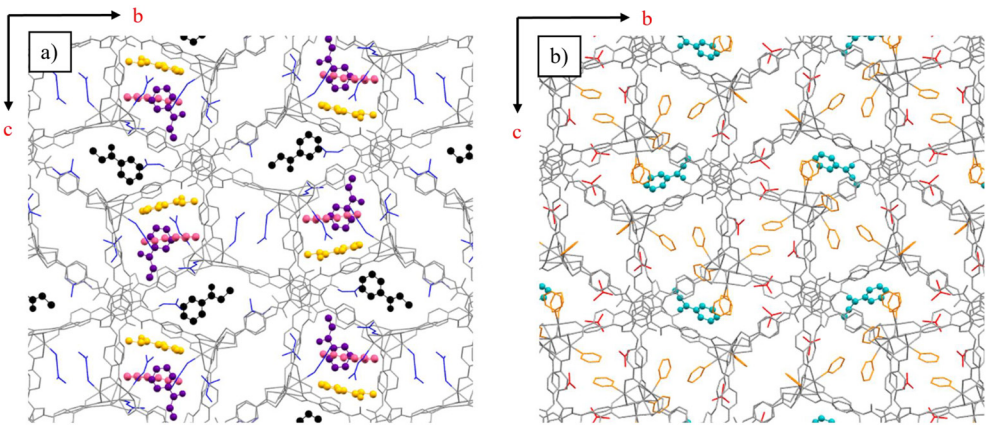

Fig. 10 Packing diagrams of complexes viewed down the *a*-axis. a) **2G**, Propiophenone in **2** b) **3G** Propiophenone in **3**, guest molecules were coloured according to their positional equivalence **2G** and **3G**. Framework displayed as capped stick in grey. DMF in blue, pyridine in orange and acetone in red. Guest molecules as ball and stick representations.

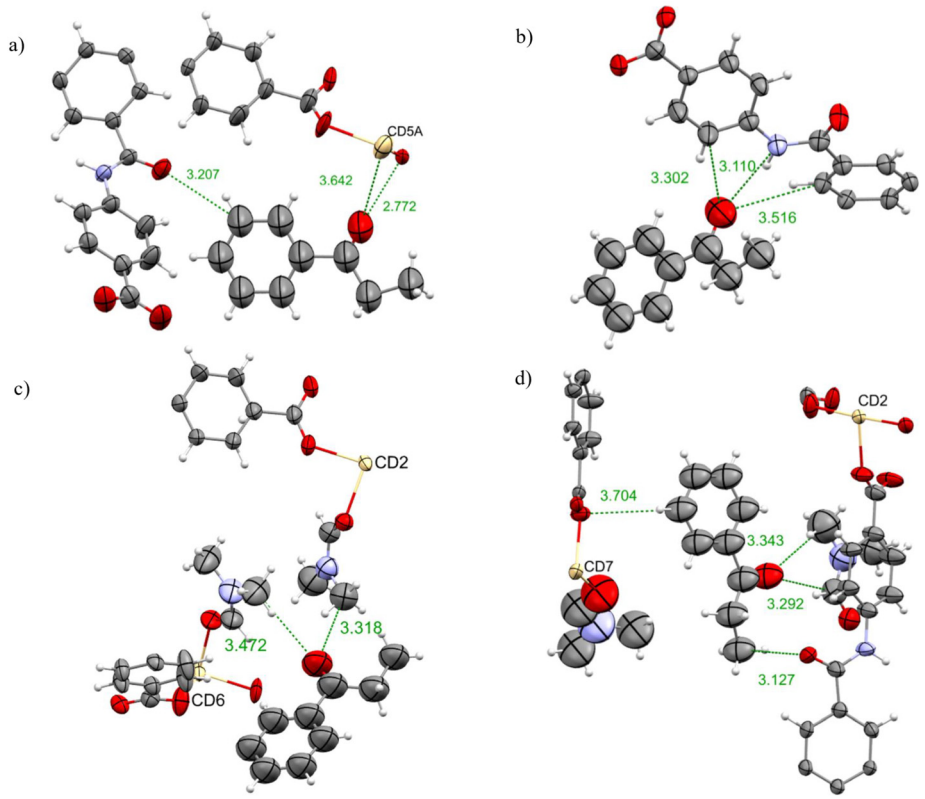

Fig. 11 a)–d) Intermolecular interactions between molecules of propiophenone found in the pores of framework **2**. Framework and guest molecules displayed as ellipsoids with 50% probability. Interaction distances are displayed in angstroms.

the framework with $C{=}O_H{\cdots}O{=}C_{framework}$ 2.77 Å. Similarly, propiophenone molecules shown in Fig. 11b–d shows the non-bonding interaction with the framework. In each case carbonyl group of the propiophenone molecules orient themselves to form hydrogen bonds with the $framework_{BTA}$, $C{=}O_H{\cdots}$framework 3.11 Å, 3.30 Å and 3.52 Å (Fig. 11b), $C{=}O_H{\cdots}framework_{DMF}$ 3.32 Å, and 3.47 Å (Fig. 11c) and $C{=}O_H{\cdots}framework_{DMF}$ 3.29 Å, and 3.34 Å.

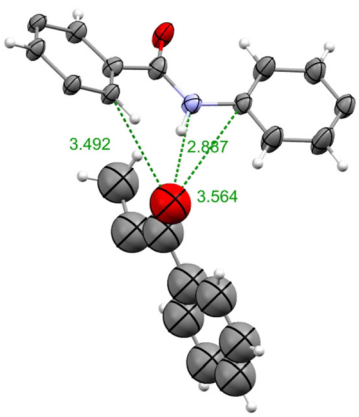

Fig. 12 Intermolecular interactions between Propiophenone molecule with the framework **3**. Framework and guest molecule displayed as ellipsoids at 50% probability. Interaction distances are displayed in angstroms.

In the inclusion complex **3G** only one molecule of propiophenone was observed in the pore shown in Fig. 10b. The propiophenone molecule is fixed *via* hydrogen bonding, $C{=}O_H{\cdots}H_{framework}$ 2.88, 3.49, 3.56 Å as shown in Fig. 12.

Conclusion

The aim of this research was to expand the CSM to a wider range of guest molecules by synthesising novel inclusion complexes and developing alternative crystalline sponges. Although sponge **1** is the most studied crystalline sponge it has practical limitations such as a hydrophobic pore environment, small pore size and instability in the presence of polar solvents and nucleophiles. Therefore, the range of guest molecules for sponge **1** is limited. Hence, to expand the CSM to a wider range of guest molecules, the development of an alternative crystalline sponge is essential. The MOF {$[Cd_7(4,4'4''$-[1,3,5-benzenetriyltris(carbonylimino)]-trisbenzoate$)_4(\mu_3\text{-}OH)_2(H_2O)_4(DMF)_4]\cdot(DMF)_7$} (**2**), with pore size 10 × 16 $Å^2$, was prepared and investigated for its utility as a crystalline sponge. Results show excellent performance of sponge **2** as a crystalline sponge which was stable in a variety of solvents (polar aprotic and polar protic) and Lewis bases. In all the inclusion complexes with these solvent molecules hydrogen bonding was observed as the dominant host-guest interaction. In addition, **2** was stable in the presence of nucleophiles and several N-containing molecules were accommodated in the sponge **2** *via*

the CAL mechanism. Sponge **2** shows versatility in accommodating guest molecules in the pores as well as *via* coordinative alignment and thus, this is a successful alternative crystalline sponge, that has overcome all the limitations of Fujita's sponge. In addition, a study was conducted to compare two closely similar structures of sponges **2** and **3**. Results revealed that sponge **3** has a relatively smaller void space for guest molecules in the pore than **2**. Perhaps surprisingly pyridine molecules bonded to Cd^{2+} ions in **3** do not form π-π interactions with the incoming guests as was hoped. The same pair of guest molecules were encapsulated in both the sponges **2** and **3** and similarities and differences in the guest binding to the framework were documented. In conclusion sponge **2** was a useful alternative sponge to **1** and is highly recommended for use in CSM, particularly to accommodate Lewis bases, nucleophile guests and for the structure determination of active pharmaceutical ingredients, as they commonly are N-containing compounds.[38,45]

3. Experimental section

Synthesis of ligand H_3BTA = 4,4′4″-[1,3,5-benzenetriyltris(carbonylimino)]-trisbenzoic acid

4,4′4″-[1,3,5-Benzenetriyltris(carbonylimino)]-trisbenzoic acid was synthesised by the reported literature procedure.[46] 1,3,5-benzenetricarboxylic acid chloride (3.98 g, 15.0 mmol) was added to a solution of 4-amino-benzoic acid (6.18 g, 45.1 mmol) and triethylamine (3.62 mL, 26.0 mmol) in *N*,*N*-dimethylacetamide (DMA) (80 mL). The mixture was stirred for 16 h at room temperature and then water (300 mL) was added. A white precipitate was formed which was filtered off and the solid was washed with acetone, water, and methanol. The product was then air-dried and characterised by NMR spectroscopy and mass spectroscopy. ^{1}H NMR (DMSO-d_6, δ ppm): 12.81 (broad peak, 3H, COOH), 10.89 (s, 3H, CONH), 8.75 (s, 3H, ArH), 7.98 (s, 12H, ArH), *m*/*z* 567.13, 100%.

Synthesis of $[Cd_7$(4,4′4″-[1,3,5-benzenetriyltris(carbonylimino)]-trisbenzoate$)_4(\mu_3$-OH$)_2(H_2O)_4(DMF)_4]\cdot$(solvent$)_7$ 2

The crystals of **2** were synthesised by a modified literature procedure.[41] A solvothermal reaction of $Cd(NO_3)_2{\cdot}6H_2O$ (0.033 g) and H_3BTA (0.013 g) in DMF (2 ml) with H_2O (4–5 drops) was performed at 85 °C for 3 days in a screw-capped pyrex vial. The colourless rod-shaped crystals of sponge **2** were obtained. The crystals were kept immersed in DMF in an incubator at 25 °C until required for the solvent exchange and guest encapsulation experiments. (Details of solvent exchange and guest encapsulation experiments are found in ESI†).

Synthesis of $[Cd_7$(4,4′4″-[1,3,5-benzenetriyltris(carbonylimino)]-trisbenzoate$)_4(\mu_3$-OH$)_2$(pyridine$)_8]\cdot$(DMF$)_2$(acetone$)_3$ 3

Sponge **3** was obtained when crystals of **2** were exchanged with diluted pyridine. When neat pyridine was used the crystal dissolved therefore pyridine was diluted with DMF. SCXRD analysis revealed that pyridine molecules replaced DMF from the coordination site but one coordinated DMF was remaining. Therefore, acetone for dilution was selected and results revealed that pyridine successful replaced DMF from all the coordination sites which is the formation of sponge **3**. Details of solvent exchange are represented in Table S1.†

Crystallographic procedures. Crystals were placed in fomblin, and single crystals were selected and mounted onto nylon loops. X-ray diffraction data were recorded at 150 K on an Agilent Super Nova dual diffractometer (Agilent Technologies Inc., Santa Clara, CA) with Cu Kα radiation (λ = 1.5418 Å). Unit cell determination, data reduction, and absorption corrections were carried out using CrysAlisPro.[47] The structures were solved by direct methods and refined by full-matrix least-squares based on F^2 using SHELX[48] within the OLEX 2.0 (ref. 49) graphical user interface. Generally, non-hydrogen atoms were refined anisotropically, and hydrogen atoms were included using a riding model but see individual reports on the refinement of guest molecules, including the modeling of disorder in the ESI.†

Author contributions

Faiza Habib did all the experiments including refinement and modelling of the crystal structures, wrote the initial draft of the article; Derek Tocher provided crystallographic advice reviewed and edited the article; Claire Carmalt provided supervision in all aspects of the paper reviewed and edited the article.

Conflicts of interest

The authors declare no competing financial interest.

Acknowledgements

The authors would like to thank University College London for Overseas Research Scholarship and Schlumberger Foundation's Faculty For the Future for funding this work.

References

1 Y. Inokuma, S. Yoshioka, J. Ariyoshi, T. Arai, Y. Hitora, K. Takada, S. Matsunaga, K. Rissanen and M. Fujita, *Nature*, 2013, **495**, 461–466.
2 Y. Inokuma, T. Ukegawa, M. Hoshino and M. Fujita, *Chem. Sci.*, 2016, **7**, 3910–3913.
3 N. Wada, R. D. Kersten, T. Iwai, S. Lee, F. Sakurai, T. Kikuchi, D. Fujita, M. Fujita and J.-K. Weng, *Angew. Chem., Int. Ed.*, 2018, **57**, 3671–3675.
4 R. D. Kersten, S. Lee, D. Fujita, T. Pluskal, S. Kram, J. E. Smith, T. Iwai, J. P. Noel, M. Fujita and J. K. Weng, *J. Am. Chem. Soc.*, 2017, **139**, 16838–16844.
5 K. Kai, M. Sogame, F. Sakurai, N. Nasu and M. Fujita, *Org. Lett.*, 2018, **20**, 3536–3540.

6 L. Rosenberger, C. von Essen, A. Khutia, C. Kühn, K. Urbahns, K. Georgi, R. W. Hartmann and L. Badolo, *Drug Metab. Dispos.*, 2020, **48**, 587–593.
7 K. Ohara and K. Yamaguchi, *Anal. Sci.*, 2020, **37**, 167–175.
8 K. Ohara, M. Kawano, Y. Inokuma and M. Fujita, *J. Am. Chem. Soc.*, 2010, **132**, 30–31.
9 M. Tominaga, T. Hyodo, Y. Maekawa, M. Kawahata and K. Yamaguchi, *Chem. – Eur. J.*, 2020, **26**, 5157–5161.
10 T. Haneda, M. Kawano, T. Kawamichi and M. Fujita, *J. Am. Chem. Soc.*, 2008, **130**, 1578–1579.
11 T. Kawamichi, T. Haneda, M. Kawano and M. Fujita, *Nature*, 2009, **461**, 633–635.
12 J. V. Knichal, H. J. Shepherd, C. C. Wilson, P. R. Raithby, W. J. Gee and A. D. Burrows, *Angew. Chem., Int. Ed.*, 2016, **55**, 5943–5946.
13 V. Duplan, M. Hoshino, W. Li, T. Honda and M. Fujita, *Angew. Chem., Int. Ed.*, 2016, **55**, 4919–4923.
14 S. Yoshioka, Y. Inokuma, V. Duplan, R. Dubey and M. Fujita, *J. Am. Chem. Soc.*, 2016, **138**, 10140–10142.
15 K. Ikemoto, Y. Inokuma, K. Rissanen and M. Fujita, *J. Am. Chem. Soc.*, 2014, **136**, 6892–6895.
16 S. Urban, R. Brkljača, M. Hoshino, S. Lee and M. Fujita, *Angew. Chem., Int. Ed.*, 2016, **55**, 2678–2682.
17 R. Brkljača, J. M. White and S. Urban, *J. Nat. Prod.*, 2015, **78**, 1600–1608.
18 Y. Matsuda, T. Mitsuhashi, S. Lee, M. Hoshino, T. Mori, M. Okada, H. Zhang, F. Hayashi, M. Fujita and I. Abe, *Angew. Chem., Int. Ed.*, 2016, **55**, 5785–5788.
19 A. D. Cardenal and T. R. Ramadhar, *ACS Cent. Sci.*, 2021, **7**, 404–414.
20 H. Sato and A. Yamano, Determining Structure of Volatile Compounds with the Crystalline Sponge Method, *Rigaku J.*, 2013, **35**, 1–3.
21 **https://www.Merckgroup.Com/En/Research/Science-Space/Presentations/Crystalline-Sponges-as-a-Sensitive-and-Rapid-Method-for-Metabolite-Identification.Html**.
22 R. D. J. Lunn, D. A. Tocher, P. J. Sidebottom, M. G. Montgomery, A. C. Keates and C. J. Carmalt, *Cryst. Growth Des.*, 2021, **21**, 3024–3036.
23 F. Habib, D. A. Tocher, N. J. Press and C. J. Carmalt, *Microporous Mesoporous Mater.*, 2020, **308**, 110548.
24 N. Zigon, V. Duplan, N. Wada and M. Fujita, *Angew. Chem., Int. Ed.*, 2021, **60**, 2–21.
25 F. Habib, D. A. Tocher and C. J. Carmalt, *Mater. Today: Proc.*, 2022, **56**, 3766–3773.
26 E. Sanna, E. C. Escudero-Adán, A. Bauzá, P. Ballester, A. Frontera, C. Rotger and A. Costa, *Chem. Sci.*, 2015, **6**, 5466–5472.
27 E. Sanna, A. Bauzá, E. C. Escudero-Adán, C. Rotger, A. Frontera and A. Costa, *Cryst. Growth Des.*, 2017, **17**, 3611–3615.
28 C. Chen, Z. Di, H. Li, J. Liu, M. Wu and M. Hong, *CCS Chem.*, 2021, **3**, 1352–1362.
29 S. Y. Zhang, L. Wojtas and M. J. Zaworotko, *J. Am. Chem. Soc.*, 2015, **137**, 12045–12049.
30 S. Y. Zhang, D. Fairen-Jimenez and M. J. Zaworotko, *Angew. Chem., Int. Ed.*, 2020, **59**, 17600–17606.
31 A. Saito, T. Sawada and M. Fujita, *Angew. Chem., Int. Ed.*, 2020, **59**, 20367–20370.
32 M. Mon, R. Bruno, J. Ferrando-Soria, L. Bartella, L. di Donna, M. Talia, R. Lappano, M. Maggiolini, D. Armentano and E. Pardo, *Mater. Horiz.*, 2018, **5**, 683–690.
33 W. de Poel, P. Tinnemans, A. L. L. Duchateau, M. Honing, F. P. J. T. Rutjes, E. Vlieg and R. de Gelder, *Chem. – Eur. J.*, 2019, **25**, 14999–15003.
34 G. H. Ning, K. Matsumura, Y. Inokuma and M. Fujita, *Chem. Commun.*, 2016, **52**, 7013–7015.
35 S. Turega, W. Cullen, M. Whitehead, C. A. Hunter and M. D. Ward, *J. Am. Chem. Soc.*, 2014, **136**, 8475–8483.
36 T. Matsumoto, R. Nakashima, A. Yamano and K. Nishino, *Biochem. Biophys. Res. Commun.*, 2019, **518**, 402–408.
37 G.-H. Ning, K. Matsumura, Y. Inokuma and M. Fujita, *Chem. Commun.*, 2016, **52**, 7013–7015.
38 F. Sakurai, A. Khutia, T. Kikuchi and M. Fujita, *Chem. – Eur. J.*, 2017, **23**, 15035–15040.
39 D. Balestri, D. Capucci, N. Demitri, A. Bacchi and P. Pelagatti, *Materials*, 2017, **10**, 1–12.
40 L. Wang, C. E. Moore and S. M. Cohen, *Cryst. Growth Des.*, 2017, **17**, 6174–6177.
41 Y. Zhang, Q. Wang, Y. J. Xiao, J. Han and X. L. Zhao, *Polyhedron*, 2012, **33**, 127–136.
42 M. Hoshino, A. Khutia, H. Xing, Y. Inokuma and M. Fujita, *IUCrJ*, 2016, **3**, 139–151.
43 Y. Inokuma, S. Yoshioka, J. Ariyoshi, T. Arai and M. Fujita, *Nat. Protoc.*, 2014, **9**, 246–252.
44 R. D. J. Lunn, D. A. Tocher, P. J. Sidebottom, M. G. Montgomery, A. C. Keates and C. J. Carmalt, *Cryst. Growth Des.*, 2020, **20**, 7238–7245.
45 L. Rosenberger, C. von Essen, A. Khutia, C. Kühn, K. Georgi, A. K. H. Hirsch, R. W. Hartmann and L. Badolo, *Eur. J. Pharm. Sci.*, 2021, **164**, 105884.
46 X. Song, Y. Zou, X. Liu, M. Oh and M. S. Lah, *New J. Chem.*, 2010, **34**, 2396–2399.
47 *CrystalisPro*, Agilent Technologies Ltd, Yarton, Oxfordshire, England, 2015.
48 G. M. Sheldrick, *Acta Crystallogr., Sect. A: Found. Crystallogr.*, 2008, **64**, 112–122.
49 O. V. Dolomanov, L. J. Bourhis, R. J. Gildea, J. A. K. Howard and H. Puschmann, *J. Appl. Crystallogr.*, 2009, **42**, 339–341.